Published in "Journal of Molecular Structure: THEOCHEM, 2010
doi: 10.1016/j.theochem.2010.03.031"
which should be cited to refer to this work.

DFT Study of the Jahn-Teller Effect in Cu(II) Chelate Complexes

Maja Gruden-Pavlović[a,b], Matija Zlatar[a], Carl-Wilhelm Schläpfer[a], Claude Daul*[,a]

[a] *Department of Chemistry, University of Fribourg, Fribourg, Switzerland*
[b] *Faculty of Chemistry, University of Belgrade, Belgrade, Serbia*

Abstract

Density Functional Theory (DFT) in conjuction with the Intrinsic Distortion Path (IDP) is employed to study the Jahn-Teller (JT) effect in all four diastereoisomers of tris(ethylenediamine)copper(II) ($[Cu(en)_3]^{2+}$) and tris(ethyleneglycol)copper(II) ($[Cu(eg)_3]^{2+}$) complexes. As a consequence of the JT effect all the isomers tetragonally elongate to the C_2 configurations. Although there are energy differences between the isomers of $[Cu(en)_3]^{2+}$, almost equal JT parameters suggest that chelate ring conformation does not have affect on the JT distortion. In a case of $[Cu(eg)_3]^{2+}$ JT effect causes additional hydrogen bond formation and these two effects define the overall geometry of isomers.

Key words: Jahn-Teller Effect, Density Functional Theory, tris(ethylenediamine)copper(II), tris(ethyleneglycol)copper(II)

1. Introduction

The Jahn-Teller (JT) theorem states that in a molecule with a degenerate electronic state, a structural distortion must occur that lowers the symmetry, removes the degeneracy and lowers the energy [1, 2]. It is familliar fact of coordination chemistry that hexacoordinated copper(II) complexes exibit a strong JT coupling. In the octahedral field five d orbitals of Cu^{2+} ion split

*Corresponding author
Email addresses: matija.zlatar@unifr.ch (Matija Zlatar), claude.daul@unifr.ch (Claude Daul)

into two groups, $(t_{2g})^6(e_g)^3$, and the complex octahedron distorts tetragonally.

The JT parameters, Fig. 1, define the adiabatic potential energy surface of the JT active compounds. It is difficult to get them experimentally, and the range of values found in literature is very wide. Thus, it is very useful to obtain theoretically the JT stabilisation energy (E_{JT}), the warping barrier (Δ) and the nuclear displacements (R_{JT}). For this purpose a multideterminental DFT procedure was devoloped in our group [3, 4]. We have performed calculations by means of this procedure on Cu(II) chelate complexes in order to study the effect caused by the central metal ion d electron degeneracy, and also to make an attempt to find a related effects caused by the JT distortion.

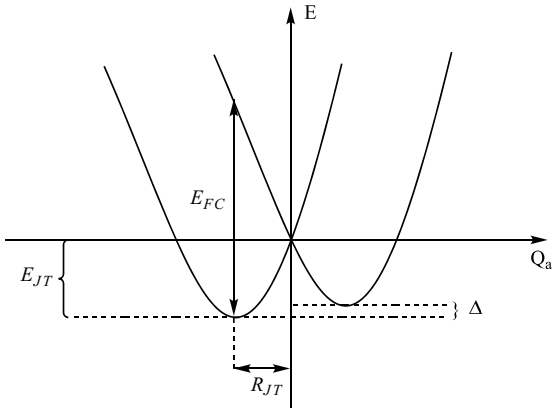

Figure 1: Indication of the JT parameters: the JT stabilisation energy, E_{JT}, the warping barrier, Δ, the JT radius, R_{JT}

In the present study we have considered all theoretically possible isomers of tris(ethylenediamine)copper(II) ($[\mathrm{Cu(en)_3}]^{2+}$) and tris(ethyleneglycol)copper (II) ($[\mathrm{Cu(eg)_3}]^{2+}$) complexes. Those complexes have four diastereoisomers, because a five membered chelate ring can adopt either δ or λ conformation, Fig. 2, and because of the overall chirality, each of these four has a mirror image structure, ending up with a total of eight isomers: $\Delta\delta\delta\delta$, $\Delta\delta\delta\lambda$, $\Delta\delta\lambda\lambda$, $\Delta\lambda\lambda\lambda$, $\Lambda\delta\delta\delta$, $\Lambda\delta\delta\lambda$, $\Lambda\delta\lambda\lambda$, $\Lambda\lambda\lambda\lambda$ [5]. Due to the identical stabilities of the enantiomers the following discussion will be limited to only the first set of four isomers of the above list.

Tris(ethylenediamine) complexes were investigated thoroughly over the

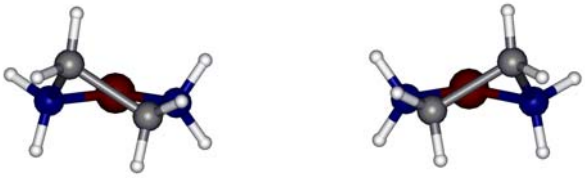

(a) δ conformation (b) λ conformation

Figure 2: Stereochemistry of five membered ethylenediamine chelate ring

years. Theoretical studies of their stereochemistry were limited in the past on the transition metals with closed shells, e.g. Co(III), and usually performed with Molecular Mechanics (MM) approach [6, 7]. Our investigation of $[Co(en)_3]^{3+}$ system shows a good ability of DFT to distinguish different stabilities of the diastereoisomers. Results obtained by DFT and MM are consistent, Table 1. Energy difference between the isomers is very small, they can all coexist in the solution, and there is rapid conversion of the δ and λ conformations [8]. A new ability of the Time Dependant Density Functional Theory (TD-DFT) to predict and explain the Circular Dichroism (CD) spectra brought again tris(ethylenediamine) complexes in a focus of interest. This is explored in the works by e.g. Ziegler at all. for the calculation of CD spectra of $[Co(en)_3]^{3+}$ [9] and $[Cr(en)_3]^{3+}$ [10], and of $[Zn(en)_3]^{2+}$ by Norani et all. [11] or Wang et all. [12] who investigated the influence of the different conformations of the chelate rings on the CD spectra of $[Ru(en)_3]^{2+}$. On the other hand, for tris(ethyleneglicol) complexes there are no computational studies so far, and they were always considered to be completely analogues to tris(ethylenediamine) complexes. Although we have already analysed $[Cu(en)_3]^{2+}$ ion as a model for macrobicyclic cage complex [13], in this work we extended the analysis of the JT effect to all four diastereoisomers. We would like to adress the question whether there is any consequence

Table 1: Energy difference between diastereoisomers of $\Delta-[Co(en)_3]^{3+}$, in kcal/mol, with Molecular Mechanics (MM) and DFT approaches (LDA, BP86, PW91)

Conformer	MM	LDA	BP86	PW91
$\delta\delta\delta$	1.82	1.29	0.68	0.75
$\delta\delta\lambda$	1.12	0.47	0.25	0.31
$\delta\lambda\lambda$	0.77	0.07	0.00	0.02
$\lambda\lambda\lambda$	0.00	0.00	0.00	0.00

of the chelate ring conformations on the JT effect in these molecules. To our knowledge this is the first detailed DFT stereochemical study of $[Cu(en)_3]^{2+}$ and $[Cu(eg)_3]^{2+}$ species.

Further motivation for this work comes from our continuous interest in systems where the JT distortion arises as a consequence of coupling of the electronic states with a number of different normal modes, so called multimode JT problem. Thus, in addition we performed the analysis of the multimode JT effect on the above mentioned systems using the method recently proposed by us [4, 14].

2. Computational Details

The DFT calculations reported in this work have been carried out using the Amsterdam Density Functional program package, ADF2007.01 [15, 16, 17]. Several studies [13, 18, 19] have shown that Local Density Approximation (LDA) tends to perform better for geometries for Werner type complexes, and that JT parameters do not depend on the functionals. Also, our results on $[Co(en)_3]^{3+}$ species demonstrate good ability of LDA to distinguish the stabilities of diastereoisomers (Table 1). Hence, LDA characterized by the Vosko-Willk-Nusair (VWN) [20] parameterization have been used for the Cu(II) complexes. For $[Co(en)_3]^{3+}$ isomers LDA and the generalized gradient approximation (GGA) with Becke exchange [21] and Perdew correlation [22] (BP86) and in the form given by Perdew-Wang (PW91) [23, 24] have been compared. All electron Triple-zeta Slater-type orbital (STO) plus one polarization function (TZP) basis set have been used for all atoms. Analytical harmonic frequencies were calculated [25, 26], and were analysed with the aid of PyVib2 1.1 [27].

Molecular Mechanics calculations were performed with the 2007/PC version of the Consistent Force Field (CFF) conformational program [28] with the parameters developed earlier [7], supplemented with a partial charges obtained from DFT calculations.

2.1. Calculation of the Jahn-Teller Parameters

Complexes under investigation have ^2E electronic ground state in the high symmetry nuclear configuration. This nuclear configuration is not a stationary point on potential energy surface, and there is coupling between the E electronic state with the non-totally symmetric, e, vibrations. The theory of this vibronic coupling, is well documented in the book by Bersuker

[2]. The adiabatic potential energy surfaces of these molecules are completely determined with the set of parameters, defined on the Fig. 1. The meaning of the parameters is clear: energy stabilization due to the JT effect is given by the value of E_{JT} (or alternatively by $E_{\mathrm{FC}} \approx 4E_{\mathrm{JT}}$), and direction and magnitude of the distortion by the R_{JT}. Recipe for the calculation of these parameters for octahedral Cu(II) complexes using multideterminental-DFT is summarized in the Fig. 3.

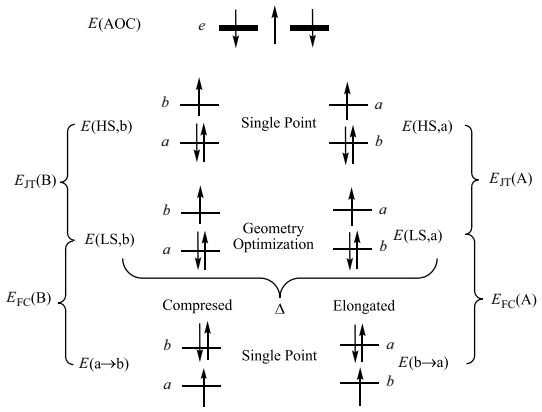

Figure 3: Multideterminental DFT aproach for the calculation of the JT parameters

This procedure consists of the following steps: i) average of configuration calculation in the high symmetry point group. This yields the geometry of the high symmetry species. In the case of octahedral Cu(II) complexes it is necessary to place 1.5 electron into each of the e orbitals, i.e. $(d_{x^2-y^2})^{1.5}(d_{z^2})^{1.5}$. ii) A single-point calculation imposing the high symmetry on the nuclear geometry and the low symmetry on the electron density. This is achieved by introducing an adequate occupation scheme of the MOs, e.g. $(d_{x^2-y^2})^2(d_{z^2})^1$. This gives the energy of a Slater determinant with an integer electron orbital occupancy. iii) A geometry optimization constraining the structure to the lower symmetry point group, with the same occupancy. E_{JT} is the difference between the energies obtained in the steps ii) and iii). Both steps are repeated for the other electronic state in the low symmetry point group. The energy of the first excited electronic state, is obtained by promoting the electron from the ground state to the first excited state for the ground state geometry. These two states differ in symmetry as indicated on Fig. 3. Energy

difference between them gives the energy of the vertical (Franck-Condon) transition E_{FC}.

2.2. Analysis of the multimode Jahn-Teller effect

In complex molecules, the JT distortion is always superposition of the number of different normal coordinates. Within the harmonic approximation the JT distortion can be analysed as a linear combination of all totally symmetric normal modes in the low symmetry minimum energy conformation. Geometry of the low symmetry (LS) energy minimum is chosen to be the origin of the configuration space, $\vec{R}_{\mathrm{LS}}$=0. Every point X on the potential energy surface can be represented by a $3N$ dimensional vector, $\vec{R}_{\mathrm{X}}$, using mass-weighted generalized coordinates relative to the origin. Within the harmonic approximation it is possible to express $\vec{R}_{\mathrm{X}}$ as a linear combination of N_{a_1} totally symmetric normal coordinates in LS:

$$\vec{R}_{\mathrm{X}} = \sum_{\mathrm{k}=1}^{N_{a_1}} w_{\mathrm{Xk}} \vec{Q}_{\mathrm{k}} \tag{1}$$

where w_{Xk} are weighting factors which represent the contribution of the displacements along the different totally symmetric normal coordinates to the $\vec{R}_{\mathrm{X}}$; $\vec{Q}_{\mathrm{k}}$ are mass-weighted totally symmetric normal coordinates, which are the eigenvectors of the Hessian, obtained by the DFT frequency calculations in the LS minimum energy conformation. The corresponding eigenvalues are λ_{k}.

Energy of the the nuclear configuration $\vec{R}_{\mathrm{X}}$, E_{X}, relative to the LS energy minimum is expressed as the sum of the energy contributions of the totally symmetric normal modes:

$$E_{\mathrm{X}} = \sum_{\mathrm{k}=1}^{N_{a_1}} E_{\mathrm{k}} = \frac{1}{2} \sum_{\mathrm{k}=1}^{N_{a_1}} w_{\mathrm{Xk}}^2 \vec{Q}_{\mathrm{k}}^2 \lambda_{\mathrm{k}} \tag{2}$$

Force at any given point (X), $\vec{F}_{\mathrm{Xk}}$ is defined as a derivate of energy over Cartesian coordinates and in the high symmetry (HS) point indicates the main driving force for the JT distortion. The total distortion force is given as a vector sum of the individual forces.

$$\vec{F}_{\mathrm{Xtot}} = \sum_{\mathrm{k}=1}^{N_{a_1}} \vec{F}_{\mathrm{Xk}} = \sum_{\mathrm{k}=1}^{N_{a_1}} w_{\mathrm{Xk}} \lambda_{\mathrm{k}} \mathbb{M}^{1/2} \vec{Q}_{\mathrm{k}} \tag{3}$$

where $\mathbb{M}$ is a diagonal $3N \times 3N$ matrix with atomic masses in triplicates as elements (m_1, m_1, m_1, m_2, ..., m_N). $\vec{F}_{\mathrm{Xtot}}$, the force which drives the nuclei to the LS minimum gives the direction from one to the another point on the adiabatic potential energy surface in a way of maximizing decrease of the energy. Path from the HS to the LS minimum obtained in this way is the Intrinsic Distortion Path (IDP), which gives additional information about the microscopic origin and mechanism of the distortion. Details about this approach has been described in our previous papers [4, 14].

3. Results and Discussion

As mentioned in the Introduction, we have investigated the four diastereoisomers for both chelate complexes ($[\mathrm{Cu(en)_3}]^{2+}$ and $[\mathrm{Cu(eg)_3}]^{2+}$). $\lambda\lambda\lambda$ and $\delta\delta\delta$ isomers exibit D_3 symmetry. The Single Occupied Molecular Orbital (SOMO) belongs to irrep. e in D_3 point group and the descent in symmetry due to the JT effect goes to C_2. Flipping the C−C backbone in one of the five-membered rings from λ to δ, or vice versa, reduces the symmetry to C_2. SOMO in these cases belongs to either a or b irrep. In order to have a comparison of the vibronic coupling in all the four isomers for $\delta\lambda\lambda$ and $\delta\delta\lambda$ geometry optimization was performed forcing both a and b orbitals to have 1.5 electrons. In this way we have obtained the geometry where the two states are accidentally degenerate, and all Cu−L bond lengths are the same. This represents quasy - D_3, high symmetry, geometry for this two isomers.

3.1. [Cu(en)$_3$]$^{2+}$

DFT calculations shows a strong evidence for the JT distortion in all diastereoisomers of $[\mathrm{Cu(en)_3}]^{2+}$. It can be clearly seen (Table 2 and Table 3) that minima on the potential energy surface for each isomer correspond to the tetragonaly elongated octahedron. Global minima is elongated $\Delta\lambda\lambda\lambda$-$[\mathrm{Cu(en)_3}]^{2+}$, with four nitrogen atoms at 2.04 Å, two nitrogen atoms at 2.47 Åfrom the central metal ion, and with trans angle at Cu^{2+} of 173°. The geometry nicely agrees with the X-ray structure [29]. In agreement with this theoretical arguments, the majority of X-ray structure determinations on tris(ethylenediamine) metal complexes revealed $\Delta\lambda\lambda\lambda$ or $\Lambda\delta\delta\delta$ configuration and none for Cu(II) mixed ring conformations, according to the Cambridge Structural Database (CSD).

Bond lengths and angles are almost the same for all the isomers, and the difference is in the sign of the torsional angle N−C−C−N. Inversion of the rings to achieve another conformation was not observed during the geometry optimization. This analysis of the geometries suggests that the JT distortion is not dependent on the conformation of the chelate rings. This is verified by the values of the JT parameters which are almost the same for all the isomers, Table 3. E_{JT} of 2.2×10^3 cm^{-1} is in agreement with experimentally determined results $2.0 \pm 0.2 \times 10^3$ cm^{-1} [30]. Energy differences between elongated forms, as well as between the regular symmetrical configuration for all the four isomers correspond to the recent theoretical investigations on tris(ethylenediamine) complexes [11, 12]. Large difference between the energies of elongated and compressed forms for each isomer, ($0.58\pm0.02\times10^3$ cm^{-1}), is a consequence of the second order JT effect, and the potential energy surfaces are warped.

In the C_2 energy minimum conformation $[\mathrm{Cu(en)_3}]^{2+}$ has 53 totally symmetric normal modes. The skeletal vibrations are coupled with the vibrations of the chelate rings and the normal coordinate analysis is complicated. Still, we are able to distinguish 4 skeletal type modes which are the most important for the distortion. Their contribution to the distortion and the contributions to the energy stabilisation are listed in Table 4. Analysis of the IDP shows that distortion starts with a breathing mode, contribution of which decreases fast along the path. Contribution of metal-ligand stretching is however increasing and dominates until 60 % of the IDP. Importance of skeletal bending increases with increasing deviation from the HS point.

Breathing mode corresponds to a_1 irrep in D_3 point group, so it does not lower the symmetry. It is interesting that distortion actually starts with this normal mode and not with metal-ligand stretching modes, which correspond to the e irrep in D_3, and which are mainly responsible for the elongation or compression of the complex octahedra. Reason for this is that breathing mode is the hardest of the skeletal modes in an octahedral arrangement [31].

Changes of the contributions of these normal modes are depicted on Fig. 4.

Table 2: Results of the DFT calculations performed to analyse the JT effect of $[Cu(en)_3]^{2+}$ chromophore, geometries are obtained with LDA; energies (LDA) are given in eV

Compound	Occupation	State	Geometry	LDA
	$e^{1.5}e^{1.5}$	^2E	D_3	-193.6050
	a^2b^1	^2B	D_3	-193.4864
	b^2a^1	^2A	D_3	-193.4918
$\delta\delta\delta$-$[Cu(en)_3]^{2+}$	a^2b^1	^2B	$C_2(B)$	-193.7591
	b^2a^1	^2A	$C_2(A)$	-193.6874
	a^1b^2	^2A	$C_2(B)$	-192.5990
	b^1a^2	^2B	$C_2(A)$	-193.0016
	$a^{1.5}b^{1.5}$	^2E	$C_2(D_3)$	-193.6282
	a^2b^1	^2B	$C_2(D_3)$	-193.5146
	b^2a^1	^2A	$C_2(D_3)$	-193.5147
$\delta\delta\lambda$-$[Cu(en)_3]^{2+}$	a^2b^1	^2B	$C_2(B)$	-193.7919
	b^2a^1	^2A	$C_2(A)$	-193.7172
	a^1b^2	^2A	$C_2(B)$	-192.5970
	b^1a^2	^2B	$C_2(A)$	-193.0407
	$a^{1.5}b^{1.5}$	^2E	$C_2(D_3)$	-193.6363
	a^2b^1	^2B	$C_2(D_3)$	-193.5120
	b^2a^1	^2A	$C_2(D_3)$	-193.5348
$\delta\lambda\lambda$-$[Cu(en)_3]^{2+}$	a^2b^1	^2B	C_2	-193.7869
	b^2a^1	^2A	C_2	-193.7171
	a^1b^2	^2A	$C_2(B)$	-192.5998
	b^1a^2	^2B	$C_2(A)$	-193.0319
	$e^{1.5}e^{1.5}$	^2E	D_3	-193.6363
	a^2b^1	^2B	D_3	-193.5205
	b^2a^1	^2A	D_3	-193.5257
$\lambda\lambda\lambda$-$[Cu(en)_3]^{2+}$	a^2b^1	^2B	$C_2(B)$	-193.7961
	b^2a^1	^2A	$C_2(A)$	-193.7251
	a^1b^2	^2A	$C_2(B)$	-192.5811
	b^1a^2	^2B	$C_2(A)$	-193.0406

Table 3: The JT parameters E_{JT}, Δ, E_{FC} are given in $\times 10^3$ cm^{-1} and R_{JT} in (amu)$^{1/2}$Å for elongated, minimum of $[Cu(en)_3]^{2+}$ species

Molecule	E_{JT}	Δ	E_{FC}	R_{JT}
$\delta\delta\delta$	2.20	0.58	9.36	2.34
$\delta\delta\lambda$	2.24	0.60	9.64	2.35
$\delta\lambda\lambda$	2.22	0.56	9.57	2.33
$\lambda\lambda\lambda$	2.22	0.57	9.80	2.34

3.2. [Cu(eg)$_3$]$^{2+}$

The JT parameters for the four isomers of $[Cu(eg)_3]^{2+}$ have been calculated from the results of multideterminental DFT calculations (Table 5) and

Table 4: Analysis of the JT multimode problem in $\lambda\lambda\lambda$-$[Cu(en)_3]^{2+}$ and by LS totally symmetric normal modes in harmonic approximation. Frequencies of selected normal modes are in cm^{-1} as obtained from ADF calculations; contribution of the normal mode $\vec{Q}_k$ to the distortion is given by c_k in %; E_i energy contribution of $\vec{Q}_k$ to the E_{JT} in %

Molecule	$\vec{Q}_k$	$\tilde{\nu}_k$ in C_2	Assignement	HS-irrep	c_k	E_i
$\lambda\lambda\lambda$-$[Cu(en)_3]^{2+}$	3	96	N−Cu−N bend	e	23.2	4.6
	4	146	Cu−N stretch	e	36.0	25.8
	6	210	Cu−N stretch	e	22.1	31.0
	12	426	breathing	a_1	2.3	11.7

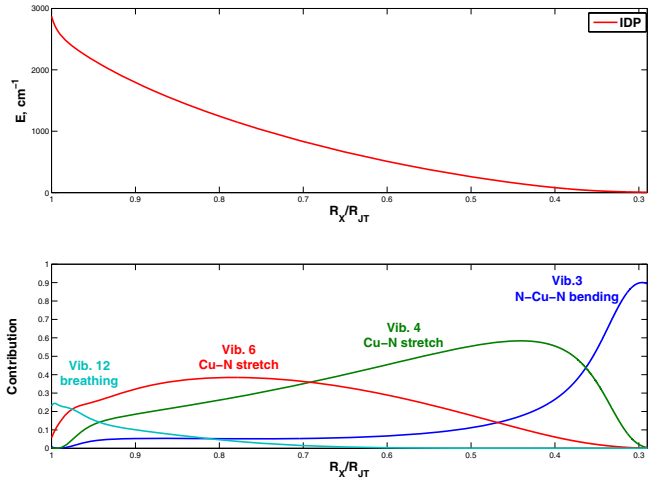

Figure 4: Changes of the contributions of the four most important normal modes to the distortion (down) along the Intrinsic Distortion Path, IDP (up) for $\lambda\lambda\lambda$-$[Cu(en)_3]^{2+}$

summarized in Table 6. The calculated order of stability for elongated, the most stable forms is: $\Delta\delta\lambda\lambda > \Delta\lambda\lambda\lambda > \Delta\delta\delta\lambda > \Delta\delta\delta\delta$. The absolute minimum is an elongated $\Delta\delta\lambda\lambda$-$[Cu(eg)_3]^{2+}$, in agreement with only two X-ray structures found in CSD [32].

On a first sight it may look surprising that we obtained larger value for E_{JT}, $1.98 - 2.42 \times 10^3 cm^{-1}$ in comparison to the experimental determination of JT parameters for the CuO_6 chromophore, $1.81 \pm 0.19 \times 10^3 cm^{-1}$ [30]. In addition, experimental evidence suggested that E_{JT} for the CuO_6 chromophore should be smaller than for the CuN_6 chromophore. Furthermore, energy differences between isomers are larger than in the case of analogues

Table 5: Results of the DFT calculations performed to analyse the JT effect of $[Cu(eg)_3]^{2+}$ chromophore, geometries are obtained with LDA; energies (LDA) are given in eV

Compound	Occupation	State	Geometry	LDA
	$e^{1.5}e^{1.5}$	^2E	D_3	-157.2514
	a^2b^1	^2B	D_3	-157.1211
	b^2a^1	^2A	D_3	-157.1265
$\delta\delta\delta$-$[Cu(eg)_3]^{2+}$	a^2b^1	^2B	$C_2(B)$	-157.4211
	b^2a^1	^2A	$C_2(A)$	-157.2961
	a^1b^2	^2A	$C_2(B)$	-156.5404
	b^1a^2	^2B	$C_2(A)$	-156.6651
	$a^{1.5}b^{1.5}$	^2E	$C_2(D_3)$	-157.3746
	a^2b^1	^2B	$C_2(D_3)$	-157.2585
	b^2a^1	^2A	$C_2(D_3)$	-157.2395
$\delta\delta\lambda$-$[Cu(eg)_3]^{2+}$	a^2b^1	^2B	$C_2(B)$	-157.5190
	b^2a^1	^2A	$C_2(A)$	-157.4708
	a^1b^2	^2A	$C_2(B)$	-156.6442
	b^1a^2	^2B	$C_2(A)$	-156.8745
	$a^{1.5}b^{1.5}$	^2E	$C_2(D_3)$	-157.5021
	a^2b^1	^2B	$C_2(D_3)$	-157.4074
	b^2a^1	^2A	$C_2(D_3)$	-157.3411
$\delta\lambda\lambda$-$[Cu(eg)_3]^{2+}$	a^2b^1	^2B	C_2	-157.6939
	b^2a^1	^2A	C_2	-157.5196
	a^1b^2	^2A	$C_2(B)$	-156.6007
	b^1a^2	^2B	$C_2(A)$	-156.9488
	$e^{1.5}e^{1.5}$	^2E	D_3	-157.5186
	a^2b^1	^2B	D_3	-157.3949
	b^2a^1	^2A	D_3	-157.3895
$\lambda\lambda\lambda$-$[Cu(eg)_3]^{2+}$	a^2b^1	^2B	C_2	-157.6354
	b^2a^1	^2A	C_2	-157.5894
	a^1b^2	^2A	$C_2(B)$	-156.7355
	b^1a^2	^2B	$C_2(A)$	-156.9505

Table 6: The JT parameters E_{JT}, Δ, E_{FC} are given in $\times 10^3$ cm^{-1} and R_{JT} in (amu)$^{1/2}$Å for elongated, minimum of $[Cu(eg)_3]^{2+}$ species

Molecule	E_{JT}	Δ	E_{FC}	R_{JT}
$\delta\delta\delta$	2.42	1.00	7.10	4.75
$\delta\delta\lambda$	2.10	0.39	7.06	4.86
$\delta\lambda\lambda$	2.31	1.41	8.82	3.36
$\lambda\lambda\lambda$	1.98	0.37	7.26	3.27

ethylenediamine complexes, and the JT parameters are distinctive.

These discrepancies are due to the orientation of the lone pair on oxygen.

In high symmetry configurations there are weak intramolecular hydrogen bonds involving H and O atoms on the λ rings. The number of hydrogen bonds decreases with a change of the ring conformation from λ to δ. Thus, in D_3 $\delta\delta\delta$ diastereoisomer hydrogen bonding is not observed. On the other hand, in all tetragonally elongated isomers hydrogen bonds are present. Stronger ones are observed in $\delta\delta\lambda$ and $\delta\lambda\lambda$ isomers. This gives a possible explanation for the encountered results. The JT effect is responsible for the different Cu−O bond lengths and enhances the intramolecular hydrogen bond formation, which causes the distortion of the angles around Cu(II) ion, Fig. 5. Due to the presence of counter ion (SO_4^{2-}), which is a better proton acceptor, only the elongation of the Cu−O bonds is observed in the crystal. Resulting geometry and energy stabilisation in the diastereoisomers is a superposition of the two effects: removal of electron degeneracy due to the JT effect and stabilization by hydrogen bond formation.

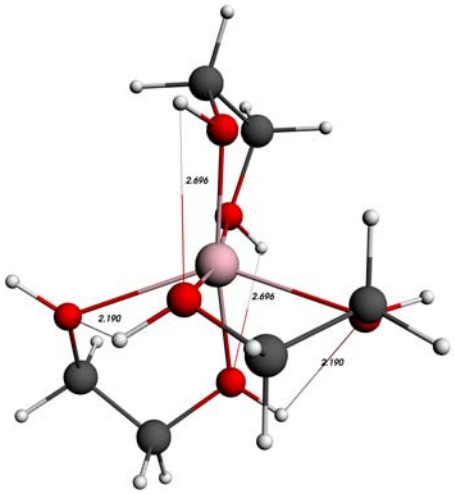

Figure 5: Optimized geometry of elongated $\delta\lambda\lambda$-$[Cu(eg)_3]^{2+}$; indication of intramolecular hydrogen bonds

In the C_2 minimum energy conformation $[Cu(eg)_3]^{2+}$ has 44 totally symmetric normal modes, but seven of them are most dominant, contributing more than 95 % to the total distortion, Table 7. Changes of the contribution of these seven modes to the distortion along the IDP are depicted in Fig.

Table 7: Analysis of the JT multimode problem in $\delta\lambda\lambda$-$[Cu(eg)_3]^{2+}$ and by LS totally symmetric normal modes in harmonic approximation. Frequencies of selected normal modes are in cm^{-1} as obtained from ADF calculations; contribution of the normal mode $\vec{Q}_k$ to the distortion is given by c_k in %; E_i energy contribution of $\vec{Q}_k$ to the E_{JT} in %

Molecule	$\vec{Q}_k$	$\tilde{\nu}_k$ in C_2	Assignement	HS-irrep	c_k	E_i
$\delta\lambda\lambda$-$[Cu(eg)_3]^{2+}$	1	21	O−Cu−O bend	e	74.3	1.8
	2	76	ring conformation	e	2.3	0.7
	3	98	O−Cu−O bend	e	2.1	1.0
	4	172	Cu−O stretch	e	5.6	8.2
	5	189	Cu−O stretch	e	2.1	5.9
	6	211	Cu−O stretch	e	7.1	22.5
	9	335	breathing	a	3.4	15.2

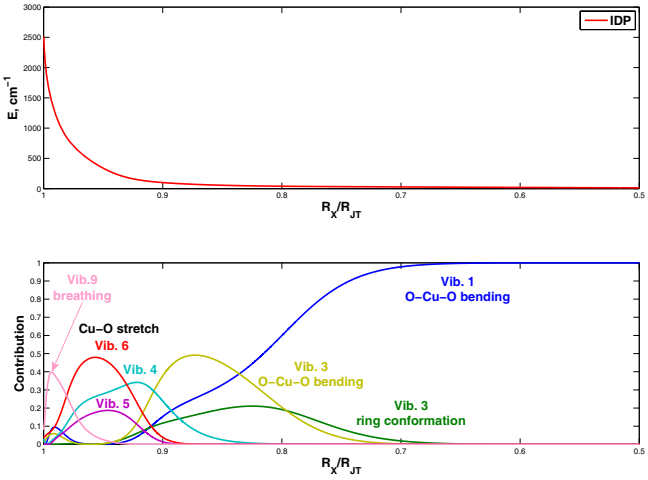

Figure 6: Changes of the contributions of the seven most important normal modes to the distortion (down) along the Intrinsic Distortion Path, IDP (up) for $\delta\lambda\lambda$-$[Cu(eg)_3]^{2+}$

6. As in the case of $[Cu(en)_3]^{2+}$ distortion starts along the breathing mode which decreases rapidly. Distortion in the second part of IDP is governed by metal-ligand stretching, typical JT active modes. When their contribution becomes lower the contribution of bending modes accompanied with conformational changes of the chelate rings increases. The IDP analysis confirms that the JT elongation of the complex octahedra enhances hydrogen bonding.

4. Conclusions

DFT is nowadays the theoretical method of choice for studying coordination compounds, i.e. Werner-type complexes. The results obtained in this work demonstrate once more the good ability of multideterminental DFT approach to predict JT parameters as well as corresponding geometries with reasonable accuracy.

As a consequence of the JT effect all four isomers of $[Cu(en)_3]^{2+}$ tetragonally elongate to the C_2 configurations. Almost equal JT parameters for all diastereisomers indicates that conformations of chelate rings do not affect the JT distortion. Tetragonal elongation is present in the case of $[Cu(eg)_3]^{2+}$ as well. We want to point out that although ethyleneglycol is analogues to the ethylendiamine ligand one should take care how far this analogy holds. The lone pair on oxygen atom in ethyleneglycol can cause some significant differences. As we have shown in this work, distortion of octahedra due to the JT effect in the case of the free ion $[Cu(eg)_3]^{2+}$, enhances the hydrogen bond formation which increases the distortion of the whole complex ion. Hence, overall stabilisation energy in this system comes from the two synergic effects: JT effect and hydrogen bond formation. Quantifying these effects will be the subject of our further work.

Acknowledgements

This work was supported by the Swiss National Science Foundation and the Serbian Ministry of Science (Grant No. 142017G). MGP acknowledges Serbian Ministry of Science for the postdoctoral fellowship during which time part of this work was done.

References

[1] H A. Jahn, E. Teller, Stability of Polyatomic Molecules in Degenerate Electronic States. I. Orbital Degeneracy, Proc. R. Soc. London, Ser A 161 (1937) 220–235.

[2] I. B. Bersuker, The Jahn-Teller Effect, Cambridge University Press, 2006.

[3] R. Bruyndockx, C. Daul, P. T. Manoharan, E. Deiss, A Nonempirical Approach to Ground-State Jahn-Teller Distortion: Case Study of VCl_4. Inorg. Chem. 36 (1997) 4251–4256.

[4] M. Zlatar, C.-W. Schläpfer, C. Daul, in H. Köppel, D. R. Yarkoni, H. Barentzen (Eds.), The Jahn-Teller-Effect Fundamentals and Implications for Physics and Chemistry, Series: Springer Series in Chemical Physics, 97 (2009) 131–165.

[5] K. A. Jensen, Tentative Proposals for Nomenclature of Absolute Configurations Concerned with Six-coordinated Complexes Based on Octahedron, Inorg. Chem. 9 (1970) 1–5.

[6] E. J. Corey, J. C. Balair, The stereochemistry of Complex Inorganic Compounds. XXII. Stereospecific Effects in Complex Ions, J. Am. Chem. Soc. 81 (1959) 2620–2628.

[7] S. R. Niketić, K. Rasmussen, Conformational Analysis of Coordination Compounds. IV. Tris(1,2-ethanediamine)- and Tris(2,3-butanediamine)cobalt(III) Complexes, Acta Chem. Scand. A 32 (1978) 391–400.

[8] Y. Saito, Inorganic Molecular Disymmetry, Springer-Verlag, Berlin-Heidelberg-New York, 1979.

[9] J. Fan, T. Ziegler, On the origin of circular dichroism in trigonal dihedral d^6 complexes of bidentate ligands containing only σ-orbitals. A qualitative model based on a density functional theory study of Λ-$[Co(en)_3]^+_3$, Chirality, 20 (2008) 938–950.

[10] J. Fan, M. Seth, J. Autschbach, T. Ziegler, Circular Dichroism of Trigonal Dihedral Chromium(III) Complexes: A Theoretical Study based on Open-Shell Time-Dependent Density Functional Theory, Inorg. Chem. 47 (2008) 11656–11668.

[11] N. Norani, H. Rahemi, S. F. Tayyari, M. J. Riley, Conformational stabilities, infrared, and vibrational dichroism spectroscopy studies of tris(ethylenediamine) zinc (II) chloride, J. Mol. Model. 15 (2009) 25-34.

[12] Y. Wang, Y. Wang, J. Wang, Y. Liu, Y. Yang, Theoretical Analysis of the Individual Contributions of Chiral Arrays to the Chiroptical Properties of Tris-diamine Ruthenium Chelates, J. Am. Chem. Soc. 131 (2009) 8839-8847.

[13] T. K. Kundu, R. Bruyndonckx, C. Daul, P. T. Manoharan, A Density Functional Approach to the Jahn-Teller Effect of $[Cu(en)_3]^{2+}$ as a Model for a Macrobicyclic Cage Complex of Copper(II), Inorg. Chem. 38 (1999) 3931–3934.

[14] M. Zlatar, C.-W. Schläpfer, E. P. Fowe, C. Daul, Density Functional Theory Study of the Jahn-Teller Effect in Cobaltocene, Pure. Appl. Chem. 81 (2009) 1397–1411.

[15] Adf2007.01. SCM, Theoretical Chemistry, Vrije Universiteit Amsterdam, The Netherlands, http://www.scm.com (2007)

[16] C. F. Guerra, J. G. Snijders, G. te Velde, E. J. Baerends, Towards an Order-n DFT Method, Theor. Chem. Acc. 99 (1998) 391–403.

[17] G. te Velde , F. M. Bickelhaupt, S. J. A. van Gisbergen, C. F. Guerra, E. J. Baerends, J. G. Snijders, T. Ziegler, Chemistry with ADF, J. Comput. Chem. 22 (2001) 931–967.

[18] M. Atanasov; P. Comba, On the Ground State $T_g \otimes e_g(T_g =^2 T_{2g},^3 T_{1g})$ Jahn-Teller-Coupling in Hexacyano complexes of $3d$ Transition Metals, J. Mol. Struct. 838 (2007) 157–163.

[19] M. Atanasov, P. Comba, C. A. Daul, A. Hauser, DFT-Based Studies on the Jahn-Teller Effect in 3d Hexacyanometalates with Orbitally Degenerate Ground States, J. Phys. Chem. A 111 (2007) 9145–9163.

[20] S. Vosko, L. Wilk, M. Nusair, Accurate Spin-Dependent Electron Liquid Correlation Energies for Local Spin Density Calculations: a Critical Analysis, Can. J. Phys. 58 (1980) 1200.

[21] A.D. Becke, Density-Functional Exchange-Energy Approximation With Correct Asymptotic Behavior, Phys. Rev. A 38 (1988) 3098–3100.

[22] J.P. Perdew, Density-Functional Approximation for the Correlation Energy of the Inhomogeneous Electron Gas, Phys. Rev. B 33 (1986) 8822-8824.

[23] J. Perdew, Y. Wang, Accurate and Simple Density Functional for the Electronic Exchange Energy: Generalized Gradient Approximation, Phys. Rev. B 33 (1986) 8800–8802.

[24] J. Perdew, J. Chevary, S. Vosko, K. Jackson, M. Pederson, D. Singh, C. Fiolhais, Atoms, molecules, solids, and surfaces: Applications of the generalized gradient approximation for exchange and correlation, Phys. Rev. B 46 (1992) 6671–6687.

[25] A. Bérces, R. M. Dickson, L. Fan, H. Jacobsen, D. Swerhone, T. Ziegler An Implementation of the Coupled Perturbed Kohn–Sham Equations: Perturbation Due to Nuclear Displacements, Comput. Phys. Commun. 100 (1997) 247–262.

[26] H. Jacobsen, A. Bérces, D. Swerhone, T. Ziegler, Analytic Second Derivatives of Molecular Energies: a Density Functional Implementation. Comput. Phys. Commun. 100 (1997) 263–276.

[27] M. Fedorovsky, Pyvib2, A Program for Analyzing Vibrational Motion and Vibrational Spectra. http://pyvib2.sourceforge.net (2007).

[28] S.R. Niketić, K. Rasmussen, The Consistent Force Field: A Documentation, Springer-Verlag, Berlin-Heidelberg (1977).

[29] D. S. Marlin, M. M. Olmstead, P.K.Mascharak, Heterolytic Cleavage of the C-C Bond of Acetonitrile with Simple Monomeric CuII Complexes: Melding Old Copper Chemistry with New Reactivity, Angew.Chem., Int.Ed., 40 (2001) 4752–4754.

[30] E. Gamp, ESR-Untersuchungen über den Jahn-Teller-Effekt in oktaedrischen Kupfer (II)-Komplexen mit trigonalen dreizähnigen Liganden, PhD Thesis, ETH Zürich, 1980.

[31] K. Nakamoto, Infrared and Raman Spectra of Inorganic and Coordination Compounds, Part II: Applications in Coordination, Organometallic, and Bioinorganic Chemistry, 5th ed. New York: Wiley, 1997.

[32] I. Labadi, L. Parkanyib, R. Grobelnyc, J. Mrozinskic, Redetermination of crystal structure, EPR and magnetic data of tris(1,2-ethanediol) copper(II) sulphate, Polyhedron, 13 (1994) 2767–2774.